

# SHORT-PERIOD AND LONG-PERIOD PERTURBATIONS OF A SPHERICAL SATELLITE DUE TO DIRECT SOLAR RADIATION

K. AKSNES

*Center for Astrophysics, Harvard College Observatory and Smithsonian Astrophysical Observatory, Cambridge, Mass. 02138, U.S.A.*

(Received 6 January, 1975)

**Abstract.** On the basis of expressions derived by Kozai, and new ones developed here, a detailed, semianalytic algorithm is presented for calculating radiation-pressure perturbations in the Keplerian elements. Through some simple modifications, the algorithm is also made to hold when  $e=0$  and/or  $i=0$ . The perturbations are obtained by summing over the sunlit segment of the satellite's orbit during each revolution or part thereof. The end points of this segment are evaluated numerically once per revolution. The effect of the inherent uncertainties in the boundaries of the Earth's shadow is discussed. The algorithm is tested by means of numerical integration of the equations of motion and through comparisons with observations of the balloon satellite 1963 30D during a 200-day interval.

## 1. Introduction

The effects of solar-radiation pressure on the motion of a spherical Earth satellite have been treated by a number of authors. Musen (1960), Parkinson *et al.* (1960), Kozai (1961), Cook (1962), and others concerned themselves only with long-period perturbations, which are obtained by averaging over the sunlit portion of the satellite's orbit. During this short interval, the perturbing force is assumed to be constant and directed away from the Sun. Musen did not take into account the Earth's shadow at all, while in the other treatments, the points of intersection of this shadow with the orbit of the satellite have been evaluated numerically. Ferraz Mello (1963), Lála and Sehnal (1969), and Lála (1970), on the other hand, approximated the discontinuous shadow equation by a continuous expansion in terms of Tchebychev series or Fourier series. Such expansions are capable of simulating the changing force due to radiation pressure during several revolutions of a satellite, as well as during the transition through the penumbral shadow. It is doubtful, however, whether this will lead to much of an improvement if the effect of the Earth's atmosphere on the shadow is not also considered, and this somewhat erratic effect probably cannot be modeled well by expansions covering several revolutions. The resulting theories include short-period as well as long-period terms. In spite of the formal elegance of these theories, for practical applications it appears more expedient and potentially more accurate to retain the shadow function in its original unexpanded form and to calculate the perturbations on a revolution-by-revolution basis. This approach is adopted in the present treatment, in which we extend Kozai's work through a detailed investigation of the short-period as well as the long-period perturbations. Though usually small, the former pertur-

bations for many satellites will considerably exceed the errors of today's high-precision satellite tracking. It is even possible that the neglect of the short-period perturbations due to radiation pressure may have caused some systematic errors in earlier air-drag analyses that were based on moderately accurate observations of balloon satellites.

## 2. The Equations of Motion

In terms of the Keplerian elements, Lagrange's variational equations take the form

$$\begin{aligned}
 \frac{da}{dt} &= 2na^3(1 - e^2)^{-1/2}F \left[ eS(v) \sin v + T(v) \frac{p}{r} \right], \\
 \frac{de}{dt} &= na^2(1 - e^2)^{1/2}F \left\{ S(v) \sin v + T(v) \left[ \cos v + \frac{1}{e} \left( 1 - \frac{r}{a} \right) \right] \right\}, \\
 \frac{di}{dt} &= na^2(1 - e^2)^{-1/2}FW \frac{r}{a} \cos u, \\
 \frac{\sin i \, d\Omega}{dt} &= na^2(1 - e^2)^{-1/2}FW \frac{r}{a} \sin u, \\
 \frac{d\omega}{dt} &= -\cos i \frac{d\Omega}{dt} + \\
 &\quad + na^2 \frac{(1 - e^2)^{1/2}}{e} F \left[ -S(v) \cos v + T(v) \left( 1 + \frac{r}{p} \right) \sin v \right], \\
 \frac{dM}{dt} &= n - 2na^2FS(v) \frac{r}{a} - (1 - e^2)^{1/2} \left( \frac{d\omega}{dt} + \cos i \frac{d\Omega}{dt} \right).
 \end{aligned} \tag{1}$$

Here,  $p = a(1 - e^2)$ ,  $v$  is the true anomaly,  $u = v + \omega$ , and  $\mu F$  ( $\mu = n^2 a^3 =$  gravitational constant times the Earth's mass) denotes the magnitude of the radiation-pressure force per unit satellite mass. This force is assumed to be acting along the Sun–Earth line, which is taken to be parallel to the Sun–satellite line. We are thus neglecting any force component normal to this line that results from an aspherical shape of the satellite or a nonuniformly reflecting surface. Nor is reradiation from the Earth and its atmosphere taken into account. Under these assumptions, we can write

$$\mu F = s \frac{A}{m} P \left( \frac{a_\odot}{r_\odot} \right)^2, \tag{2}$$

where  $A/m$  is the cross-sectional area-to-mass ratio of the satellite,  $P$  ( $\approx 4.65 \times 10^{-5}$  dyn cm $^{-2}$ ) is the force per unit area exerted at the Earth by the Sun when its geocentric distance  $r_\odot$  is equal to its mean distance  $a_\odot$ , and  $s$  is a constant whose value lies between 0 and 2, depending on the reflection characteristics of the satellite's surface. Furthermore,  $S(v)$ ,  $T(v)$ , and  $W$  are the direction cosines of the force  $\mu F$  along the

satellite's radius vector  $r$ , perpendicular to  $r$  in the orbital plane, and along the orbit normal, respectively (Kozai, 1961):

$$\begin{aligned} \begin{Bmatrix} S(v) \\ T(v) \end{Bmatrix} = & -\cos^2 \frac{i}{2} \cos^2 \frac{\varepsilon}{2} \begin{Bmatrix} \cos \\ \sin \end{Bmatrix} (\lambda_{\odot} - u - \Omega) - \\ & -\sin^2 \frac{i}{2} \sin^2 \frac{\varepsilon}{2} \begin{Bmatrix} \cos \\ \sin \end{Bmatrix} (\lambda_{\odot} - u + \Omega) - \\ & -\frac{1}{2} \sin i \sin \varepsilon \left[ \begin{Bmatrix} \cos \\ \sin \end{Bmatrix} (\lambda_{\odot} - u) - \begin{Bmatrix} \cos \\ \sin \end{Bmatrix} (-\lambda_{\odot} - u) \right] - \\ & -\sin^2 \frac{i}{2} \cos^2 \frac{\varepsilon}{2} \begin{Bmatrix} \cos \\ \sin \end{Bmatrix} (-\lambda_{\odot} - u + \Omega) - \\ & -\cos^2 \frac{i}{2} \sin^2 \frac{\varepsilon}{2} \begin{Bmatrix} \cos \\ \sin \end{Bmatrix} (-\lambda_{\odot} - u - \Omega), \end{aligned} \quad (3)$$

$$\begin{aligned} W = & \sin i \cos^2 \frac{\varepsilon}{2} \sin (\lambda_{\odot} - \Omega) - \\ & -\sin i \sin^2 \frac{\varepsilon}{2} \sin (\lambda_{\odot} + \Omega) - \cos i \sin \varepsilon \sin \lambda_{\odot}, \end{aligned}$$

where  $\varepsilon$  denotes the obliquity of the ecliptic, and  $\lambda_{\odot}$ , the ecliptic longitude of the Sun. The quantities  $\varepsilon$ ,  $\lambda_{\odot}$ , and  $a_{\odot}/r_{\odot}$  can be computed with sufficient accuracy from the expressions (see *Explanatory Supplement to the Astronomical Ephemeris* 1961, p. 98)

$$\begin{aligned} d &= \text{MJD} - 15\,019.5, \\ \varepsilon &= 23^{\circ}44', \\ M_{\odot} &= 358^{\circ}48' + 0^{\circ}985\,600\,27 \text{ d}, \\ \lambda_{\odot} &= 279^{\circ}70' + 0^{\circ}985\,647\,34 \text{ d} + 1^{\circ}92 \sin M_{\odot}, \\ \frac{a_{\odot}}{r_{\odot}} &= \frac{1 + 0.016\,72 \cos (M_{\odot} + 1^{\circ}92 \sin M_{\odot})}{0.999\,72}, \end{aligned} \quad (4)$$

where MJD is the Modified Julian Day.

### 3. Expressions for the Perturbations

Equations (1) can be integrated if all the variables on the right-hand side, except those depending explicitly on  $v$ , are held constant.\* Kozai (1961) obtained the following expressions (we take the opportunity here to correct three misprints that occurred in

\* In spite of this approximation, tests show that the accuracy of Equations (5a) is improved by evaluating the secularly changing quantities  $S$ ,  $T$ ,  $W$ , and  $\omega$  at the times  $t(E_1)$  and  $t(E_2)$ , rather than by holding them constant during this interval.

them) for the perturbations suffered by a satellite that moves in sunlight from eccentric anomaly  $E_1$  to  $E_2$  (add  $2\pi$  to  $E_2$  below if  $E_2 < E_1$ ):

$$\begin{aligned}
\delta a &= 2a^3 F \left| S \cos E + T(1 - e^2)^{1/2} \sin E \right|_{E_1}^{E_2}, \\
\delta e &= a^2 F (1 - e^2)^{1/2} \left| \frac{1}{4} S(1 - e^2)^{1/2} \cos 2E + \right. \\
&\quad \left. + T \left( \frac{3}{2} E - 2e \sin E + \frac{1}{4} \sin 2E \right) \right|_{E_1}^{E_2}, \\
\delta i &= a^2 F W (1 - e^2)^{-1/2} \left| \left[ -\frac{3}{2} eE + (1 + e^2) \sin E - \frac{e}{4} \sin 2E \right] \cos \omega + \right. \\
&\quad \left. + (1 - e^2)^{1/2} \left( \cos E - \frac{e}{4} \cos 2E \right) \sin \omega \right|_{E_1}^{E_2}, \\
\sin i \delta \Omega &= a^2 F W (1 - e^2)^{-1/2} \times \\
&\quad \times \left| \left[ -\frac{3}{2} eE + (1 + e^2) \sin E - \frac{e}{4} \sin 2E \right] \sin \omega - \right. \\
&\quad \left. - (1 - e^2)^{1/2} \left( \cos E - \frac{e}{4} \cos 2E \right) \cos \omega \right|_{E_1}^{E_2}, \tag{5a} \\
\delta \omega &= -\cos i \delta \Omega + \frac{a^2 F (1 - e^2)^{1/2}}{e} \left| S \left( -\frac{3}{2} E + e \sin E + \frac{1}{4} \sin 2E \right) + \right. \\
&\quad \left. + T(1 - e^2)^{-1/2} \left( e \cos E - \frac{1}{4} \cos 2E \right) \right|_{E_1}^{E_2}, \\
\delta M &= -(1 - e^2)^{1/2} (\delta \omega + \cos i \delta \Omega) - \\
&\quad - 3a^2 F \left| S \left[ -\frac{3}{2} eE + \left( \frac{5}{3} + \frac{2}{3} e^2 \right) \sin E - \frac{5}{12} e \sin 2E \right] - \right. \\
&\quad - T(1 - e^2)^{1/2} \left( \frac{5}{3} \cos E - \frac{5}{12} e \cos 2E \right) - \\
&\quad \left. - [S \cos E_1 + T(1 - e^2)^{1/2} \sin E_1] (E - e \sin E) \right|_{E_1}^{E_2},
\end{aligned}$$

where  $S = S(0)$ ,  $T = T(0)$ , and  $W$  are given by Equations (3) with  $v = 0$ . The expression for  $\delta M$  differs from Kozai's in that we have performed the integration  $-\frac{3}{2} \int (\delta a/a) dM$ . Note that this integral will also contribute a term  $\delta M = -\frac{3}{2} (\delta \bar{a}/a) \Delta M$ , where  $\delta \bar{a}$  is the change in  $a$  per revolution, when the satellite moves through an arc  $\Delta M$  in the Earth's shadow. The other elements then remain constant.

The expressions for  $\delta \omega$  and  $\delta M$  are singular for  $e = 0$ , although the sum  $\delta \omega + \delta M$  remains well-defined, since its  $e$  divisor can be removed simply by expanding the factor  $1 - (1 - e^2)^{1/2} = \frac{1}{2} e^2 + O(e^4)$ . This difficulty can be overcome by computing the per-

turbations directly in the radius vector and in the argument of latitude when the eccentricity gets below, say,  $a\sqrt{F}$ :

$$\begin{aligned}\delta r &= r \frac{\delta a}{a} - a \cos v \delta e + a(1 - e^2)^{-1/2} \sin v e \delta M, \\ \delta u &= \delta \omega + \frac{a^2}{r^2} (1 - e^2)^{1/2} \delta M + (2 + e \cos v) \sin v \delta e (1 - e^2)^{-1} \\ &= \delta \omega + \delta M + \left[ \frac{3}{2}e + (2 + 3e^2) \cos v + e \cos^2 v + O(e^3) \right] e \delta M + \\ &\quad + (2 + e \cos v) \sin v (1 - e^2)^{-1} \delta e.\end{aligned}\quad (5b)$$

A similar problem with  $\delta\Omega$  and  $\delta\omega$  for very small inclinations can be avoided by using the following for the perturbations in latitude  $\theta$  and longitude  $\phi$  if  $\sin i < a\sqrt{F}$ :

$$\begin{aligned}\cos \theta \delta \theta &= \sin u \cos i \delta i + \cos u \sin i \delta u, \\ \delta \phi &= \delta \Omega + \cos i \delta u [1 + \sin^2 i \sin^2 u + O(\sin^4 i)] - \\ &\quad - \frac{\sin i \tan u}{1 + \cos^2 i \tan^2 u} \delta i,\end{aligned}\quad (5c)$$

in which the appropriate expression above for  $\delta u$  should be substituted. It follows that  $\delta\Omega$  and  $\delta\omega$  will appear only in the combinations  $\delta\Omega + \cos i \delta\omega$  and  $\sin i \delta\omega$ , both of which are nonsingular at  $i=0$  and can easily be computed with the aid of Equations (5a).

From these equations, we can obtain both the long-period terms summed over complete revolutions and the short-period terms during part of a revolution in sunlight between arbitrary limits  $E_1$  and  $E_2$ . During one revolution, measured from one shadow exit to the next, the net changes in the orbital elements are given by

$$\begin{aligned}\delta \bar{a} &= \delta a(E_1, E_2), \\ \delta \bar{e} &= \delta e(E_1, E_2), \\ \delta \bar{i} &= \delta i(E_1, E_2), \\ \delta \bar{\Omega} &= \delta \Omega(E_1, E_2) + \Delta \dot{\Omega}, \\ \delta \bar{\omega} &= \delta \omega(E_1, E_2) + \Delta \dot{\omega}, \\ \delta \bar{M} &= \delta M(E_1, E_2) - \frac{3}{2} \frac{\delta \bar{a}}{a} (E - e \sin E) \Big|_{E_2}^{E_1} + \Delta \dot{M},\end{aligned}\quad (6)$$

where  $E_1$  and  $E_2$  (add  $2\pi$  to  $E_2$  if  $E_2 < E_1$ ) here denote the eccentric anomalies at shadow exit and shadow entry, respectively, and  $\Delta \dot{\Omega}$ ,  $\Delta \dot{\omega}$ , and  $\Delta \dot{M}$  are the *accumulated* changes in the gravitational rates (rad/rev)  $\dot{\Omega}$ ,  $\dot{\omega}$ , and  $\dot{M}$  due to the interaction of radiation pressure and the Earth's attraction:

$$\Delta \dot{\Omega} = 3\pi \sum J_2 \frac{R^2}{p^2} \left[ \cos i \left( \frac{7}{4} \frac{\delta \bar{a}}{a} - 2 \frac{e}{1 - e^2} \delta \bar{e} \right) + \frac{1}{2} \sin i \delta \bar{i} \right],$$

$$\begin{aligned} \Delta\dot{\omega} = 3\pi \sum J_2 \frac{R^2}{p^2} \left[ (1 - 5 \cos^2 i) \left( \frac{7}{8} \frac{\delta\bar{a}}{a} - \frac{e}{1 - e^2} \delta\bar{e} \right) - \right. \\ \left. - \frac{5}{2} \cos i \sin i \delta\bar{i} \right], \end{aligned} \quad (7)$$

$$\begin{aligned} \Delta\dot{M} = 3\pi \sum \left\{ J_2 \frac{R^2}{p^2} (1 - e^2)^{1/2} \left[ (1 - 3 \cos^2 i) \left( \frac{7}{8} \frac{\delta\bar{a}}{a} - \frac{3}{4} \frac{e}{1 - e^2} \delta\bar{e} \right) - \right. \right. \\ \left. \left. - \frac{3}{2} \cos i \sin i \delta\bar{i} \right] - \frac{\delta\bar{a}}{a} \right\}. \end{aligned}$$

In the above,  $R$  is the equatorial radius and  $J_2$  is the dynamical oblateness of the Earth. Only the first-order oblateness terms have been included, but they ought to be sufficient for the present purpose. The summation is extended over the number of revolutions since the initial epoch to which the perturbations are referred.

Care must be exercised in evaluating the eccentric anomalies  $E_1$  and  $E_2$  of shadow exit and entry. The maximum error  $\Delta E$  tolerated in these quantities can best be judged by studying, over many revolutions, the behavior of the semimajor axis, which is of crucial importance because of its accumulative effect on the mean anomaly. Since the expression (5a) for  $\delta a$  does not contain a secular term proportional to  $E$ , the net change  $\delta\bar{a}$  in  $a$  after one revolution will usually be a small difference between two much larger numbers representing the short-period perturbations at the shadow boundaries; yet the maximum error in  $\delta\bar{a}$  will be essentially proportional to  $\Delta E$  times the amplitude of the short-period oscillation in  $a$ . If we, in turn, multiply by the number of revolutions in the interval considered, we arrive at an estimate for the maximum error in  $a$  at the end of the interval. To illustrate this, let us anticipate some results from Section 5: For the balloon satellite 1963 30D (Dash 2), we find an average  $\delta\bar{a} = -1.5 \text{ m rev}^{-1}$  over a period of 200 days ( $\sim 1715 \text{ rev}$ ), while the average amplitude of the short-period oscillations in  $a$  is roughly 150 m. To maintain an accuracy of, say, 50 m, we then obtain  $\Delta E = 50/150/1715 \text{ rad} = 0.001$ .

The smallness of this tolerance in  $E_1$  and  $E_2$ , as well as the discontinuity in the radiation-pressure force at these points in the orbit, probably explains why several investigators have experienced difficulties in maintaining accuracy when calculating the perturbations due to this force by means of numerical integration. The discontinuity problem can be overcome by letting the force vary from zero at the inner edge of the penumbra to a maximum at the outer edge. As for the theory, if this force variation is assumed to be linear, the penumbra is automatically accounted for by referring the umbral limits  $E_1$  and  $E_2$  to the center of the Sun. Apart from any residual effect of the penumbra, refraction and clouds in the Earth's atmosphere will have an appreciable influence on the size and shape of the shadow. While these effects are difficult to model, that of the Earth's flattening can easily be accounted for. Unless all these effects are incorporated, the inherent uncertainties in the calculated values of  $E_1$  and  $E_2$  are likely to be much larger than 0.001. It would seem well worth the effort to

establish these uncertainties, and to try to improve on the calculation of  $E_1$  and  $E_2$  accordingly, by means of visual timings or photometric observations of a satellite's entry into and exit from the Earth's shadow.

The angles  $E_1$  and  $E_2$  can be determined explicitly by solving a quartic in  $\sin E$  or  $\cos E$ , provided the orbit of the satellite is kept fixed during the interval  $t(E_2) - t(E_1)$  and the Earth's shadow is assumed to have a cylindrical shape. These restrictions can be removed if the shadow boundaries are instead determined by a step-by-step search along the orbit. Besides giving more precise values for  $E_1$  and  $E_2$ , this method can probably also be made more efficient than the explicit one.

The satellite will be in shadow if

$$S(v) > 0 \quad \text{and} \quad P(E) \equiv R_e - r\sqrt{1 - S^2(v)} > 0, \quad (8)$$

where  $S(v) = S \cos v + T \sin v$  and  $R_e$  denotes the radius of the shadow ellipse in the plane containing the Sun and the radius vector  $r$  of the satellite. The radius  $R_e$  depends on the Earth's equatorial radius  $R$  and flattening  $f$ , and on the declinations  $\delta_\odot$  and  $\delta$  of the Sun and the satellite, as follows:

$$R_e = R \left[ 1 - \frac{f(\sin \delta + S(v) \sin \delta_\odot)^2}{1 - S^2(v)} \right], \quad (9)$$

where

$$\sin \delta = \sin i \sin u,$$

$$\sin \delta_\odot = \sin \varepsilon \sin \lambda_\odot.$$

Passage into or out of the shadow will be accompanied by a change of sign of the function  $P(E)$ , whose two real roots (provided the entire orbit is not in sunlight)  $E_1$  and  $E_2$  can be determined conveniently by the so-called *regula falsi* method. In order to eliminate a needless search, we can use the fact that the satellite will be sunlit throughout its orbit if (but not only if)  $a(1 - e) > R_e/|W|$ . Once the shadow boundaries have been found for one revolution, they can be determined for subsequent revolutions in just a few iterations.

#### 4. How to Apply the Theory

Let us assume that a set of mean elements  $a, e, i, \Omega, \omega, M$  and the rates  $\dot{\Omega}, \dot{\omega}, \dot{M}$  are given for an initial epoch  $t_0$  and we wish to compute the perturbations for a later or earlier time  $t$ . These rates should approximate as closely as possible the actual mean rates during the interval  $t - t_0$ , excluding the effects of radiation pressure. The exact definition of the elements is otherwise essentially an external problem since the first-order perturbations calculated from Equations (5) to (7) are not sensitive to small changes in the elements.

The application of the theory can be conveniently broken down into the following steps:

(1) By means of Equations (5), the perturbations in the elements are computed for the interval between  $t_0$  and the time of the nearest shadow exit.

(2) From Equations (6), with the aid of Equations (5) and (7), the long-period perturbations are computed and added up over as many complete revolutions through consecutive shadow exits as required to reach the final time  $t$ . The elements should be updated after each revolution.

(3) A final application of Equations (5) will yield the short-period perturbations for any remaining fraction of a revolution.

(4) Summing the perturbations computed in the preceding three steps will give the total perturbations in the elements due to radiation pressure during the interval  $t - t_0$ .

These steps have been programmed in FORTRAN for an electronic computer. The program RADPR, which requires about 3000 octal computer words on a CDC 6400 machine, is available from the author upon request.

### 5. Tests of the Theory

With a view to practical applications, the following questions naturally arise: (a) To what accuracy do the preceding formulas represent a true solution of the equations of motion (1)? (b) How well can the solution be expected to account for the observed motions of actual, 'nonideal' satellites under the influence of radiation pressure? (c) What kind of improvements or extensions of the theory may be possible?

The first question can be answered with a fair degree of certainty through comparisons with numerically integrated solutions of Equations (1). For a direct comparison with the theory, such integrations must be performed with the secular rates due to  $J_2$  (Brouwer, 1959) added onto expressions (1) for  $d\Omega/dt$ ,  $d\omega/dt$ , and  $dM/dt$ . For this comparison, we have chosen the balloon satellite 1963 30D (Dash 2), whose well-observed motion can also provide an answer to the second question raised above. The initial conditions have been adopted from an analysis by Slowey (1974):

$$\text{epoch} = \text{MJD } 38\,400.0,$$

$$a = 10.085\,44 \text{ Mm},$$

$$e = 0.025\,422,$$

$$i = 88^\circ 39' 24",$$

$$M = 0.956\,23 + 8.572\,99(t - 38\,400)(\text{rev}),$$

$$\omega = 227^\circ 49' 3" - 0^\circ 9' 83.08(t - 38\,400),$$

$$\Omega = 45^\circ 38' 12.4" - 0^\circ 5' 6.38(t - 38\,400),$$

$$s = 1.105,$$

$$A/m = 37.9 \text{ cm}^2 \text{ g}^{-1}.$$

The perturbations in the six orbital elements, according to both the theory and the



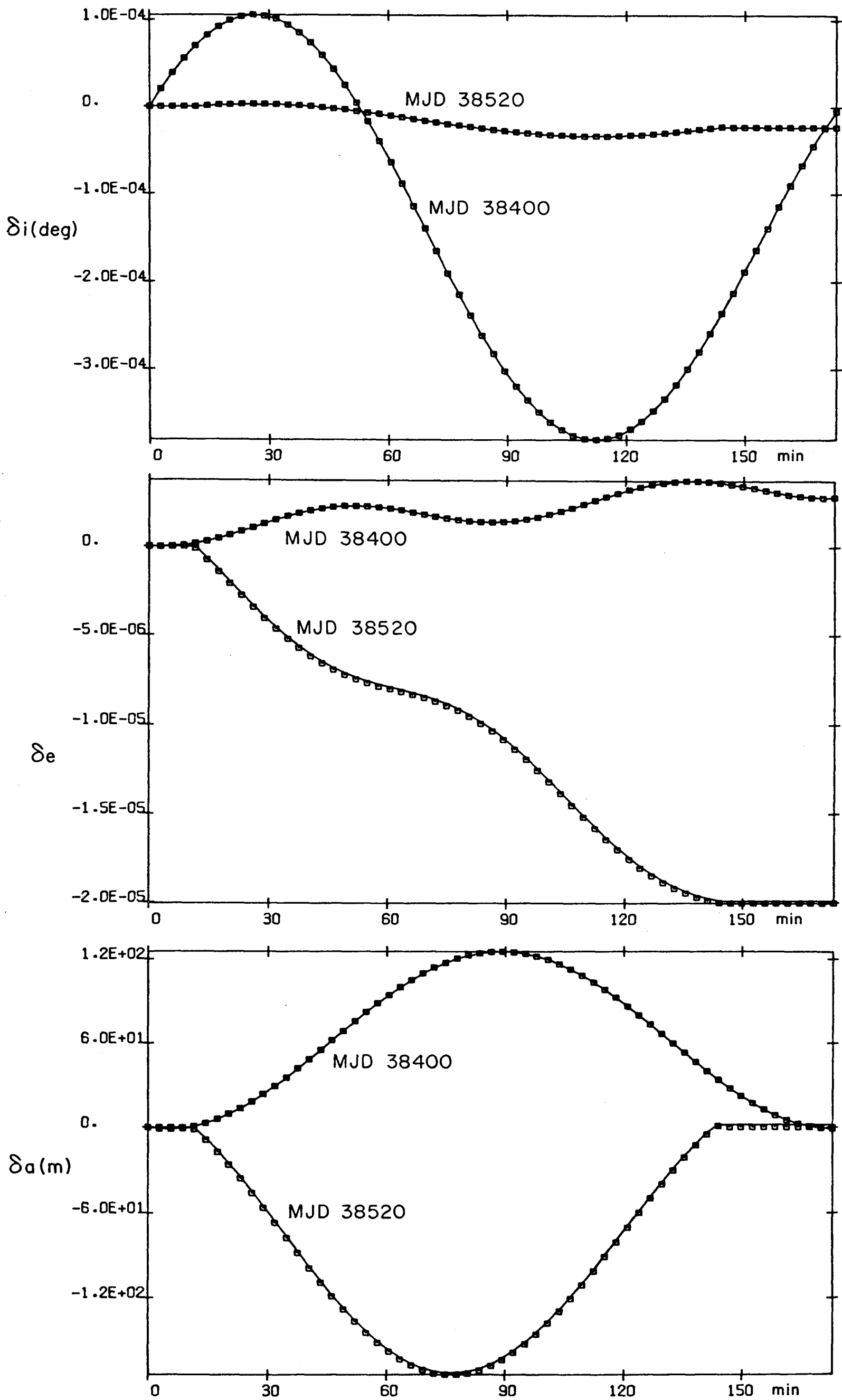


Fig. 1. Perturbations in  $a$ ,  $e$ , and  $i$  due to direct solar radiation during one revolution of 1963 30D measured from MJD 38400 and MJD 38520. The continuous curves represent the theory, and the squares, the numerical integration.

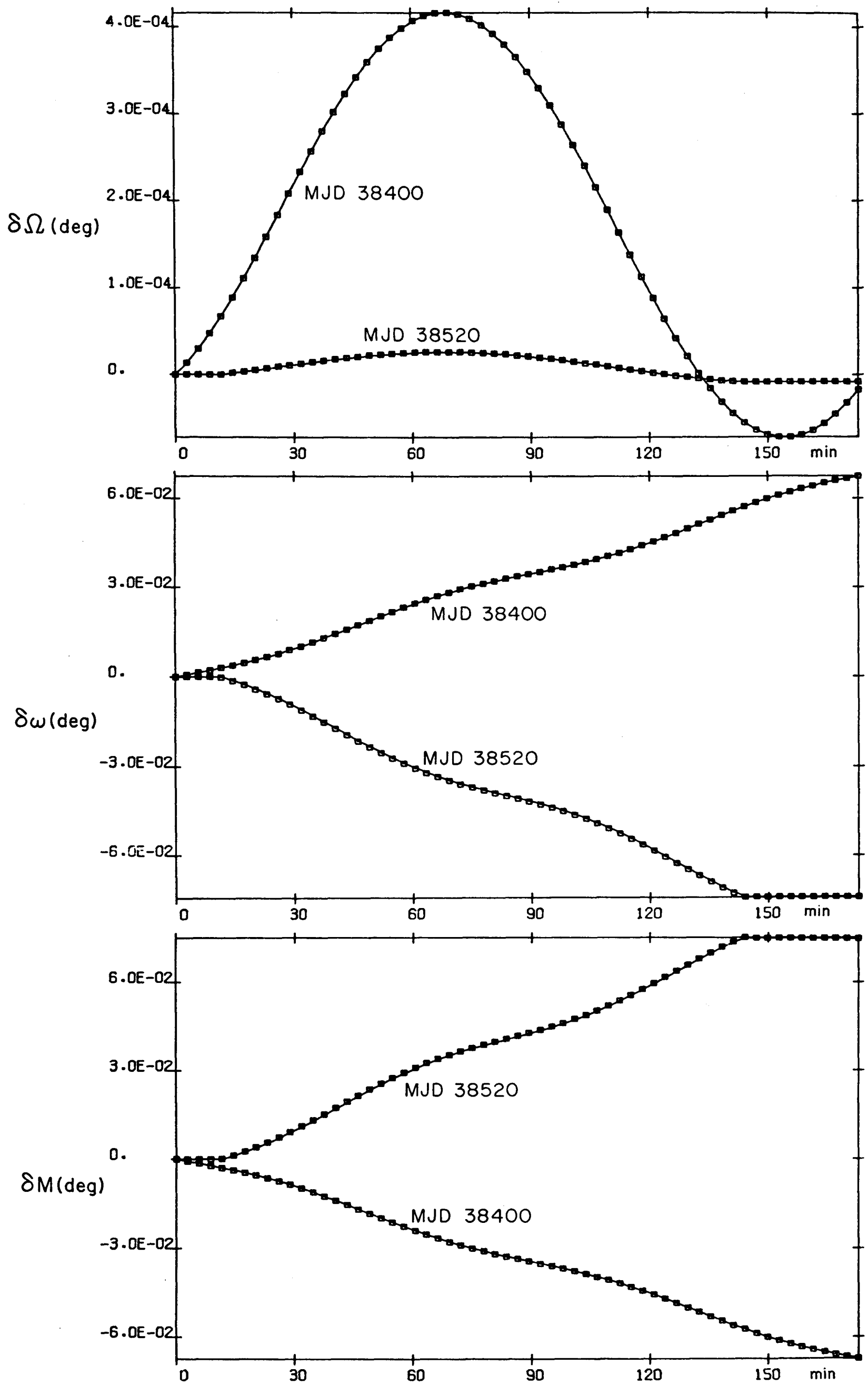


Fig. 2. Perturbations in  $M$ ,  $\omega$ , and  $\Omega$  corresponding to those in  $a$ ,  $e$ , and  $i$  in Figure 1.

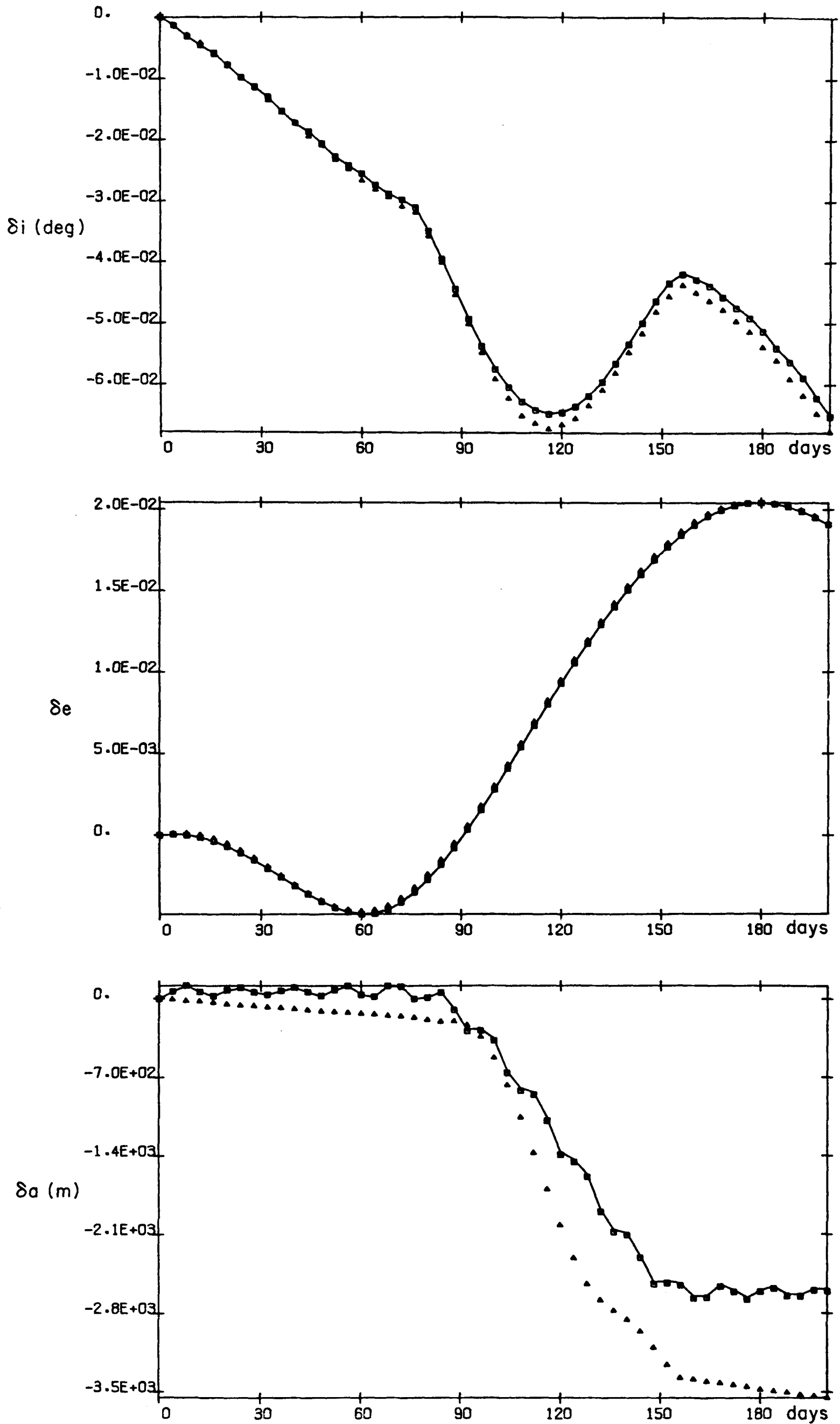


Fig. 3. Perturbations in  $a$ ,  $e$ , and  $i$  of 1963 30D due to direct solar radiation during a 200-day period beginning at MJD 38400. The continuous curves represent the theory; the squares, the numerical integration; and the triangles, the observations.

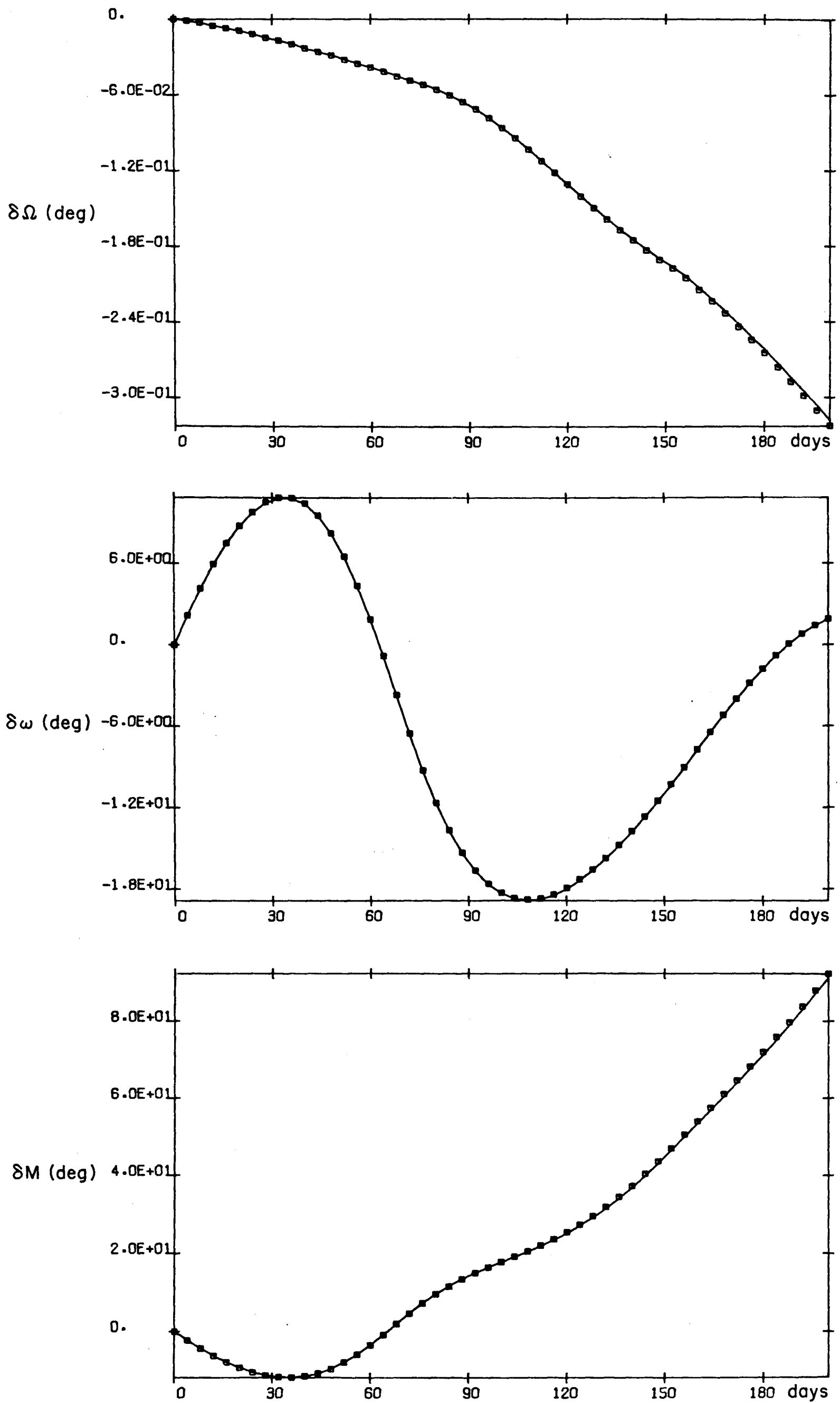


Fig. 4. Perturbations in  $M$ ,  $\omega$ , and  $\Omega$  corresponding to those in  $a$ ,  $e$ , and  $i$  in Figure 3, but without the comparison with observations.

integration, are plotted vs time in Figures 1 and 2 for one revolution of the satellite (168 min) for MJD 38 400 and MJD 38 520. At the earlier date, the satellite did not enter the Earth's shadow, so there was no net change in  $a$ , in accord with Equation (5a) for  $\delta a$ . During the first 12 min and the last 30 min of the revolution starting at MJD 38 520, the satellite was immersed in the Earth's shadow, as can be inferred from the corresponding horizontal portions of the curves in Figures 1 and 2. In the cases considered here, and for a variety of other orbits we have investigated, the theory and numerical integration were found to agree to within a fraction of a percent during one revolution.

With a maximum amplitude of about 175 m, the short-period oscillations of 1963 30D might be detectable in the precisely reduced Baker-Nunn observations of this satellite. Comparisons with observations of the computed short-period perturbations would require the elimination of a number of other perturbations from the observed positions. In an air-drag analysis from 1963 30D, Slowey (1974) has made a very satisfactory comparison of this kind for the long-period perturbations due to radiation pressure. However, in view of the above results, it is conceivable that the neglect of the short-period effects of radiation pressure might have introduced some small systematic errors in the derived mean elements. Only if the observations are distributed randomly over the orbit – which was probably not the case – would these errors tend to cancel. The short-period perturbations due to radiation pressure, though relatively unimportant in the case of 1963 30D, have an amplitude of about 600 m for the balloon satellite 1966 56A (Pageos) and, as such, are far from negligible.

Figures 3 and 4 show the agreement between theory and integration for 1963 30D for a 200-day interval. In Figure 3, we also plot the perturbations in  $a$ ,  $e$ , and  $i$  due to direct solar radiation, as deduced by Slowey from the available observations. The corresponding perturbations in the elements  $M$ ,  $\omega$ , and  $\Omega$  are not readily available, because of the difficulty of separating out the secular changes that result in these elements from disturbing forces other than radiation pressure and its interaction with the Earth's oblateness. The three different curves for  $\delta e$  are in nearly perfect agreement, while the observational curve for  $\delta i$  deviates slightly from the two nearly coincident curves representing the theory and the integration. The rather pronounced deviation of the observational curve for  $\delta a$  indicates the presence of some small secular variations in  $a$  not due to radiation pressure. This is particularly evident for the portions of the curve covering the first 76 and the last 44 days. During these intervals, the satellite was continuously in sunlight, and there should be no net change in  $a$ , in accordance with the integrated and theoretical curves for  $\delta a$ . The agreement between theory and integration is again quite satisfactory. The corresponding curves for  $\delta a$  both show some fairly regular and closely matched 16-day oscillations (the theoretical curve connects points 4 days apart by straight lines). These are the short-period perturbations of Figure 1, which, by coincidence, are sampled in such a way that they exhibit a 'beat' period of 15.98 days (137 rev). In view of the fact that the satellite made 1715 revolutions during the 200-day interval, it is remarkable that the theory preserves both the

phase and the amplitude of the short-period oscillations so well. Of course, the indicated precision of about 25 m in  $a$  at the end of this interval cannot be attained in practice unless the actual locations of the shadow boundaries are evaluated to a very high degree of accuracy, taking into account the various anomalous effects discussed in Section 3.

Figures 5 and 6 plot the differences ( $\Delta a$ ,  $\Delta e$ ,  $\Delta i$ ,  $\Delta M$ ,  $\Delta \omega$ , and  $\Delta \Omega$ ) between the theoretical and the integrated perturbations of Figures 3 and 4. Not surprisingly, the curves on Figure 6 for  $\Delta \omega$  and  $\Delta \Omega$ , and especially for  $\Delta M$ , show secular trends caused by minute differences in the rates  $\dot{M}$ ,  $\dot{\omega}$ , and  $\dot{\Omega}$ . This is to be expected in an initial-value problem involving so many satellite revolutions. About two-thirds of the perturbation in  $M$  at the end of the 200-day interval reflects changes in  $a$  (cf. Equations (7)). Although the discrepancies in  $a$  amount to a maximum of 25 m, and most of the time are considerably smaller, they nevertheless cause a gradual buildup of almost  $1^\circ$  in  $M$ . In many applications, the mean rates of the angles  $M$ ,  $\omega$ , and  $\Omega$  are to be determined from observations. The secular parts of  $\Delta M$ ,  $\Delta \omega$ , and  $\Delta \Omega$ , as represented by the regression lines labeled  $\Delta \bar{M}$ ,  $\Delta \bar{\omega}$ , and  $\Delta \bar{\Omega}$  on Figure 6, would in such a case be absorbed; the maximum discrepancies in  $M$  and  $\Omega$  are thereby reduced by more than 50%.

In summary, it appears that the theory, insofar as the simplifying conditions on which it is based are fulfilled, is capable of an accuracy of 1% or better. In spite of the need to evaluate the expressions for the perturbations once per revolution, the theory affords a tremendous savings of computer time over a straight numerical inte-

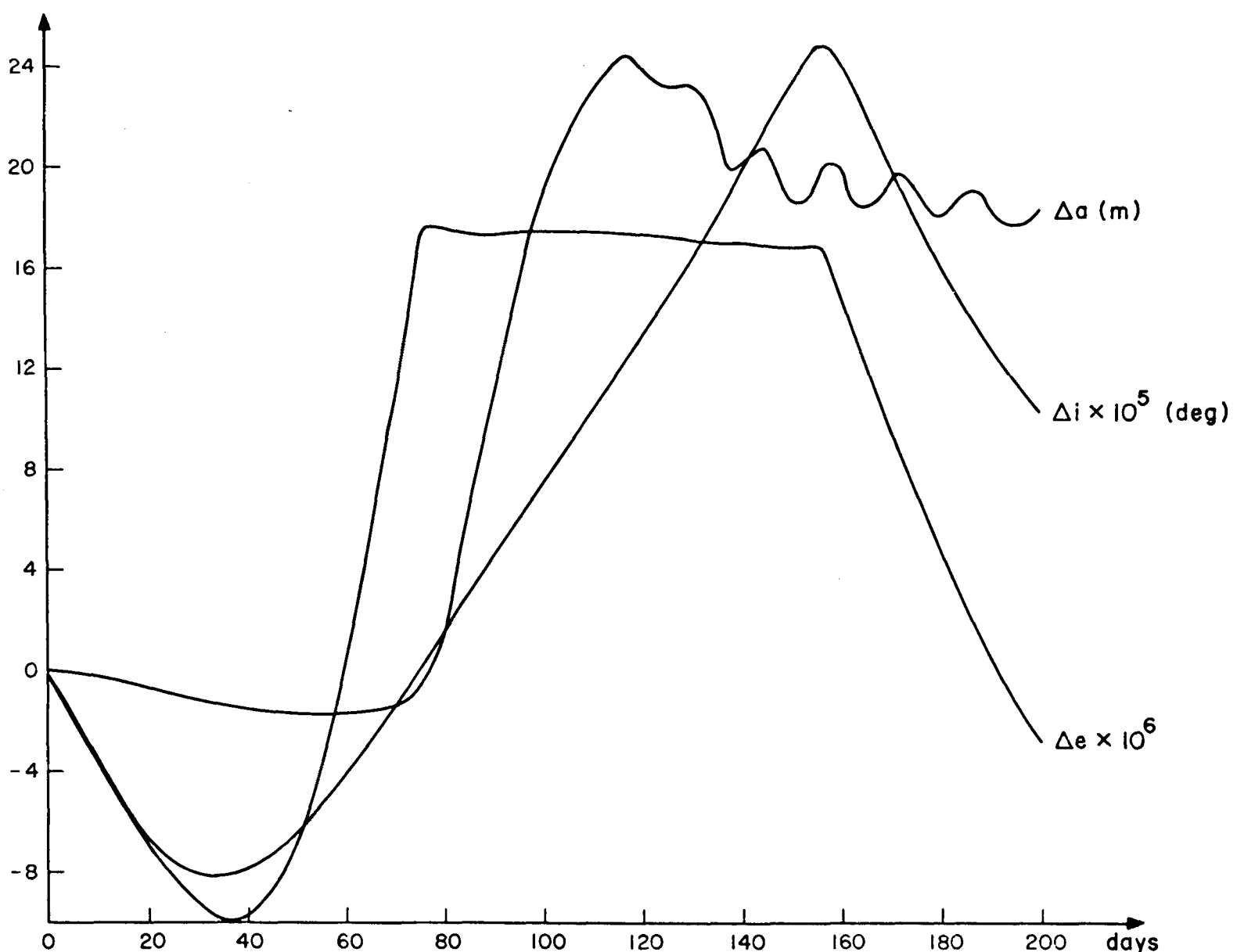


Fig. 5. Differences ( $\Delta a$ ,  $\Delta e$ ,  $\Delta i$ ) between the theoretical and the integrated curves on Figure 3.

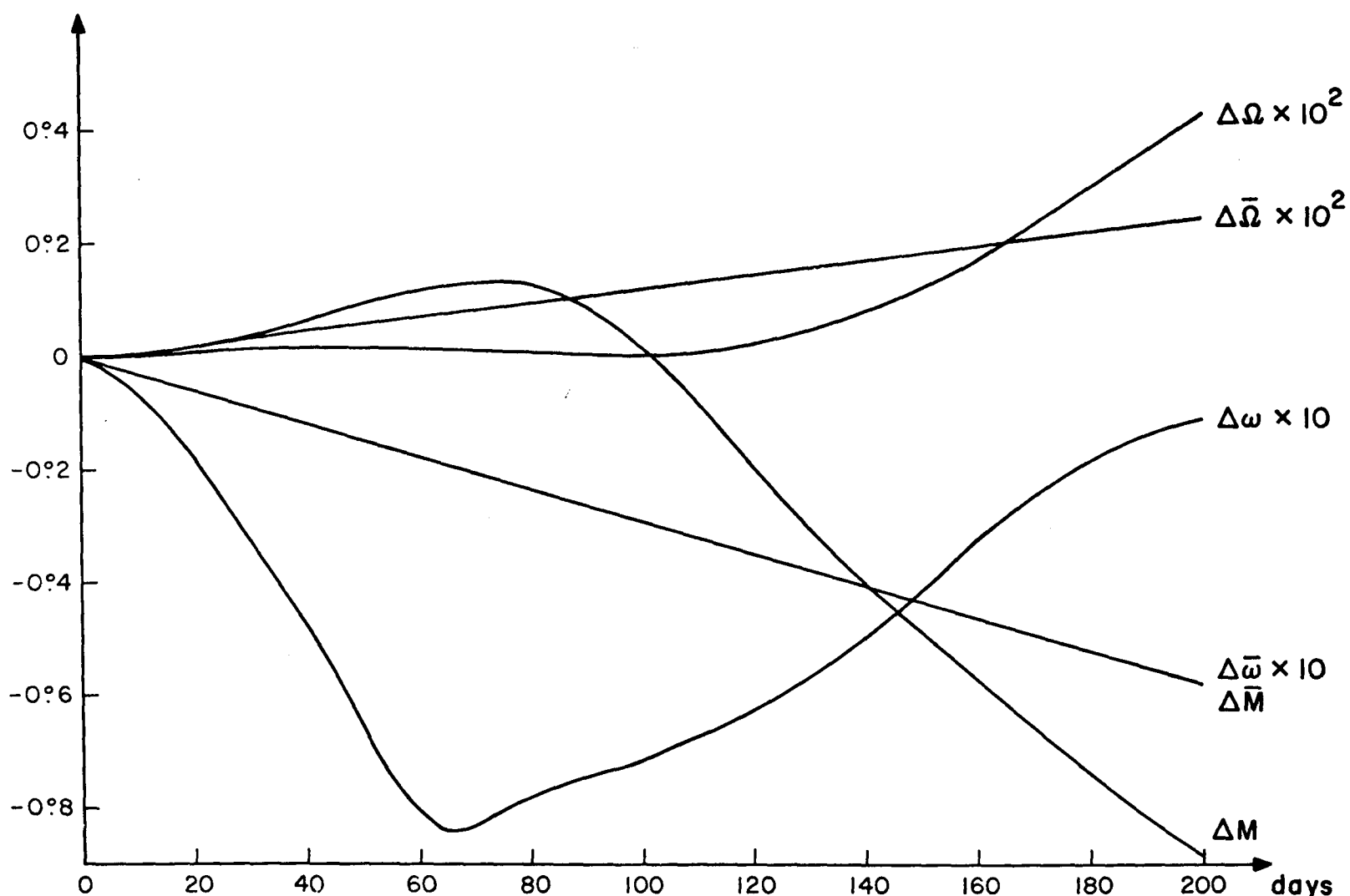


Fig. 6. Differences ( $\Delta M$ ,  $\Delta\omega$ ,  $\Delta\Omega$ ) between the theoretical and the integrated curves on Figure 4.  $\Delta\bar{M}$ ,  $\Delta\bar{\omega}$ , and  $\Delta\bar{\Omega}$  represent the secular parts of the differences.

gration. For the example just considered (1715 rev), the calculations took 70 min ( $\sim 200\,000$  steps) for the integration but only 20 s for the theory, on a CDC 6400 computer. Turning now to the third question raised above, we shall briefly investigate to what extent the simplifying conditions may not be met for typical satellites.

Analyses by Fea and Smith (1970) and Slowey (1974) have shown that the motion of 1963 30D is noticeably perturbed by radiation reflected from the Earth and by transverse forces arising from the slightly aspherical shape of the satellite. The asphericity appears to be even more pronounced for 1966 56A (Smith and Kissell, 1971). Although the resulting perturbations of 1963 30D amount to only a few percent of those plotted on Figures 3 and 4 (direct radiation pressure only), Slowey found their inclusion necessary in order to satisfy the observations. While Slowey used a fully numerical method to account for perturbations due to reradiation from the Earth, Lautman (1974) has constructed a semianalytic theory for computing them under somewhat simplifying conditions. Lucas (1974) has derived exact expressions for forces arising from radiation both incident on and reflected from a prolate spheroid. It might be possible to introduce those expressions into Equations (1) and then perform an approximate integration to obtain semianalytic expressions for the perturbations in the elements.

#### Acknowledgement

This work was supported in part by Grant NGR 09-015-002 from the National Aeronautics and Space Administration.

## References

- Brouwer, D.: 1959, *Astron. J.* **64**, 378.
- Cook, G. E.: 1962, *Geophys. J.* **6**, 271.
- Fea, K. H. and Smith, D. E.: 1970, *Planetary Space Sci.* **18**, 1499.
- Ferraz Mello, S.: 1963, in *Proceedings of XIV<sup>e</sup> Congrès Intern. d'Astronaut., Paris*, p. 41.
- Kozai, Y.: 1961, *Smithsonian Astrophys. Obs. Spec. Rep. No.* 56.
- Lála, P.: 1970, *Bull. Astron. Inst. Czech.* **22**, 63.
- Lála, P. and Sehnal, L.: 1969, *Bull. Astron. Inst. Czech.* **20**, 327.
- Lautman, D. A.: 1974, personal communication.
- Lucas, J. R.: 1974, National Oceanic and Atmospheric Administration, *Tech. Rep. No.* 61.
- Musen, P.: 1960, *J. Geophys. Res.* **65**, 1391.
- Parkinson, R. W., Jones, H. M., and Shapiro, I. I.: 1960, *Science* **131**, 920.
- Slowey, J. W.: 1974, *Smithsonian Astrophys. Obs. Spec. Rep. No.* 356.
- Smith, D. E. and Kissell, K. E.: 1971, *Goddard Space Flight Center Doc.* X-553-71-338.